

# **$^{13}\text{CO}(J = 1 - 0)$ DEPRESSION IN LUMINOUS STARBURST MERGERS, REVISITED**

Yoshiaki Taniguchi<sup>1</sup>, Youichi Ohyama<sup>1</sup>, & D. B. Sanders<sup>2</sup>

<sup>1</sup>Astronomical Institute, Tohoku University, Aoba, Sendai 980-8578, Japan

<sup>2</sup>Institute for Astronomy, University of Hawaii, 2680 Woodlawn Drive, Honolulu, HI 96822

Received \_\_\_\_\_; accepted \_\_\_\_\_

## ABSTRACT

It is known that merging galaxies with luminous starbursts and high far-infrared luminosities tend to have higher  $R_{1-0} = {}^{12}\text{CO}(J=1-0)/{}^{13}\text{CO}(J=1-0)$  integrated line intensity ratios ( $R_{1-0} \simeq 20 - 50$ ) than normal spiral galaxies ( $R_{1-0} \simeq 5 - 15$ ). Comparing far-infrared luminosities [ $L(\text{FIR})$ ] with those of  ${}^{12}\text{CO}(J=1-0)$  and  ${}^{13}\text{CO}(J=1-0)$  for a sample of normal and starburst galaxies, Taniguchi & Ohyama found that the observed high  $R_{1-0}$  values for the luminous starburst mergers are attributed to their lower  ${}^{13}\text{CO}$  line intensities by a factor of 3 on the average. They suggested the following two possibilities; in the luminous starburst mergers, 1)  ${}^{13}\text{CO}$  is underabundant with respect to  ${}^{12}\text{CO}$ , or 2) excitation and/or optical depth effects are responsible for the change in  $R_{1-0}$ . In this paper, we investigate the second possibility using higher transition data of both  ${}^{12}\text{CO}$  and  ${}^{13}\text{CO}$  emission lines. Applying the same method proposed by Taniguchi & Ohyama to both  ${}^{12}\text{CO}(J=2-1)$  and  ${}^{13}\text{CO}(J=2-1)$ , we find that  ${}^{13}\text{CO}(J=2-1)$  is also depressed with respect to  ${}^{12}\text{CO}(J=2-1)$ . This suggests that the  ${}^{13}\text{CO}$  gas may be underabundant in the high- $R_{1-0}$  starburst mergers although we cannot rule out the possibility that excitation and optical depth effects are still affecting  $R_{2-1}$ , for example due to the large velocity widths in the CO emission lines. Additional observations of both  ${}^{12}\text{CO}$  and  ${}^{13}\text{CO}$  lines at  $J \geq 3$  are required to better constrain the conditions of the molecular gas in luminous starburst galaxies.

*Subject headings:* galaxies: emission lines - galaxies: starburst - interstellar: molecules

## 1. INTRODUCTION

Since starburst phenomena affect both the chemical evolution of galaxies and the physical conditions of the interstellar medium in galaxies, an understanding of starburst activity is one of the important issues in astrophysics. Starbursts occur in dense molecular gas clouds which are generally located in the central regions of galaxies. Massive stars formed in the starbursts provide a negative feedback to the parent and ambient molecular gas clouds in the form of intense radiation fields and strong stellar winds as well as subsequent supernova explosions. Therefore it is important to investigate the molecular gas properties of starburst galaxies (Young & Scoville 1991; Henkel, Mauersberger, & Baan 1991; Sanders & Mirabel 1996 and references therein).

One of the interesting properties of molecular gas in starburst galaxies is that galaxy mergers with luminous starbursts (i.e.,  $L(\text{FIR}) \gtrsim 10^{11} L_\odot$ : hereafter luminous starburst mergers) tend to have higher  $R_{1-0}$  ( $\equiv I^{[12\text{CO}(J=1-0)]}/I^{[13\text{CO}(J=1-0)]}$ ) integrated line intensity ratios than normal spiral galaxies (Aalto et al. 1991, 1995, 1997; Casoli et al. 1991; Casoli, Dupraz, & Combes 1992a, 1992b; Hurt & Turner 1991; Turner & Hurt 1992; Garay, Mardones, & Mirabel 1993; Henkel & Mauersberger 1993; Henkel et al. 1998). One possible explanation for the higher  $R_{1-0}$  values is that they are due to the inflow of disk gas with high  $^{12}\text{C}/^{13}\text{C}$  abundance ratios, possibly combined with a  $^{12}\text{C}$  enhancement caused by nucleosynthesis in massive stars (e.g., Henkel et al. 1998). However, recently, Taniguchi & Ohyama (1998a; hereafter TO98) have compared far-infrared luminosities [ $L(\text{FIR})$ ] with CO luminosities,  $L^{[12\text{CO}(J=1-0)]}$  and  $L^{[13\text{CO}(J=1-0)]}$ , for a sample of normal and starburst galaxies, and have found that the observed higher  $R_{1-0}$  values are associated almost exclusively in the luminous starburst mergers and appear to be attributed to a lower intensity of  $^{13}\text{CO}(J=1-0)$  with respect to  $^{12}\text{CO}(J=1-0)$  when compared to normal galaxies. TO98 suggested either that  $^{13}\text{CO}$  is underabundant with respect to  $^{12}\text{CO}$ , or that

the  $^{13}\text{CO}(1-0)$  level population is more depressed relative to  $^{12}\text{CO}(1-0)$  due to excitation and/or optical depth effects, leading to the high  $R_{1-0}$  in the luminous starburst mergers studied in their paper. In this paper, we investigate the second possibility using available higher transition data of both  $^{12}\text{CO}$  and  $^{13}\text{CO}$  emission lines.

## 2. $^{12}\text{CO}(J=2-1)/^{13}\text{CO}(J=2-1)$ INTEGRATED LINE INTENSITY RATIO

TO98 demonstrated that the comparison of  $L(\text{FIR})$  with both  $L[^{12}\text{CO}]$  and  $L[^{13}\text{CO}]$  provides a powerful tool for understanding the origin of the high- $R_{1-0}$  in luminous starburst mergers (see also Taniguchi & Ohyama 1998b). If the observed high  $R_{1-0}$  values are attributed to excitation and optical depth effects, for example higher gas kinetic temperatures and/or denser gas clouds, then this could possibly be discerned in the measured values of  $R_{2-1}$  or, if necessary, in even higher transition line ratios. In order to examine if this is the case, we investigate the excitation properties of both  $^{12}\text{CO}$  and  $^{13}\text{CO}$  molecules for a sample of normal and starburst galaxies using data currently available from the literature.

We have compiled  $^{12}\text{CO}(J=2-1)$  and  $^{13}\text{CO}(J=2-1)$  integrated intensities from Aalto et al. (1995) and Casoli et al. (1992b). The integrated intensity ratio  $I[^{12}\text{CO}(J=2-1)]/I[^{13}\text{CO}(J=2-1)]$  is referred as  $R_{2-1}$ . Our sample consists of 24 galaxies and includes objects with extreme infrared luminosities such as the ultraluminous infrared galaxy Arp 220. These integrated intensities are then used to compute CO luminosities;  $L(\text{CO})$  is defined as  $L(\text{CO}) = A \times I(\text{CO}) \text{ K km s}^{-1} \text{ pc}^2$  where  $A$  is the observed area in units of  $\text{pc}^2$  and  $I(\text{CO}) = \int T_A^* \eta^{-1} dv \text{ K km s}^{-1}$  where  $T_A^*$  is the observed antenna temperature corrected for atmospheric extinction and  $\eta$  is the main beam efficiency.

The FIR data are compiled from the *IRAS* Faint Source Catalog (Moshir et al. 1992). The FIR luminosities are estimated using  $L(\text{FIR}) = 4\pi D^2 1.26 \times 10^{-11} [2.58 \times S(60) + S(100)]$

(ergs s<sup>-1</sup>) where  $S(60)$  and  $S(100)$  are the *IRAS* 60  $\mu$ m and 100  $\mu$ m fluxes in units of Jy and  $D$  is the distance (Helou, Soifer, & Rowan-Robinson 1985). Distances of nearby galaxies are taken from the Nearby Galaxies Catalog (Tully 1988); distances of other galaxies are estimated using a Hubble constant  $H_0 = 75$  km s<sup>-1</sup> Mpc<sup>-1</sup> with  $V_{\text{GSR}}$  (recession velocity with respect to the Galactic Standard of Rest) given in de Vaucouleurs et al. (1991). The compiled data are given in Table 1. All of the data presented here have been corrected for beam-size (see Aalto et al. 1995; Casoli et al. 1992b). Although our sample is not statistically complete, it is the largest sample compiled so far. TO98 defined the class of high- $R_{1-0}$  galaxies by adopting the criterion of  $R_{1-0} \geq 20$ . Using this limit, the present sample contains the following seven high- $R_{1-0}$  objects; NGC 1614, NGC 3256, NGC 4194, NGC 6240, Arp 220, Arp 299, and IRAS 18293–3413.

In Figure 1, we compare  $L[{}^{12}\text{CO}(J=2-1)]$  with  $L[{}^{13}\text{CO}(J=2-1)]$ . For reference, we also show the comparison between  $L[{}^{12}\text{CO}(J=1-0)]$  and  $L[{}^{13}\text{CO}(J=1-0)]$  in the left panel which is taken from TO98. Although two high- $R_{1-0}$  galaxies, NGC 4194 and NGC 6240, have significantly lower  $L[{}^{13}\text{CO}(J=2-1)]$  with respect to  $L[{}^{12}\text{CO}(J=2-1)]$ , the remaining galaxies have  $R_{2-1}$  ratios within the upper range (i.e.  $\sim 10$ –30) found for  $R_{1-0}$ .

In Figure 2, we compare  $L(\text{FIR})$  with both  $L[{}^{12}\text{CO}(J=2-1)]$  and  $L[{}^{13}\text{CO}(J=2-1)]$ .  $L[{}^{12}\text{CO}(J=2-1)]$  appears to be correlated with  $L(\text{FIR})$  (in an integrated intensity versus flux plot, i.e. after removing the the  $D^2$  effect from Figure 2, there is a good correlation), but the scatter is larger than observed for the correlation between  $L[{}^{12}\text{CO}(J=1-0)]$  and  $L(\text{FIR})$  (TO98). On the other hand, the correlation between  $L(\text{FIR})$  and  $L[{}^{13}\text{CO}(J=2-1)]$  is poorer than that between  $L(\text{FIR})$  and  $L[{}^{12}\text{CO}(J=2-1)]$  because the majority of the high- $R_{1-0}$  galaxies have lower  $L[{}^{13}\text{CO}(J=2-1)]$  by a factor of 3 than what would be expected from the correlation for the normal- $R_{1-0}$  galaxies. Thus, we find that both  ${}^{12}\text{CO}(J=2-1)$  and  ${}^{13}\text{CO}(J=2-1)$  show similar behavior as observed in the  $J=1-0$  transition (TO98). In

order to show this more clearly, we present a diagram of  $R_{1-0}$  versus  $R_{2-1}$  for our sample in Figure 3. In Table 2, we summarize the statistical properties for both the high- $R_{1-0}$  and the “normal- $R_{1-0}$ ” galaxies.

### 3. $^{12}\text{CO}(J=3-2)/^{13}\text{CO}(J=3-2)$ INTEGRATED LINE INTENSITY RATIO

Published measurements of extragalactic  $^{13}\text{CO}(J=3-2)$  emission are available only for M82 (Tilanus et al. 1991; Wild et al. 1992) and IC 342 (Wall & Jaffe 1990). Tilanus et al. (1991) obtained  $^{13}\text{CO}(J=3-2)$  spectra at three positions in M82; the center and the two peaks of the circumnuclear ring located  $\pm 12$  arcsec from the center using the 15 m JCMT with a beam size of 14 arcsec (FWHM). They obtained  $R_{3-2} \simeq 15$  for the nucleus while  $\simeq 10$  for the circumnuclear ring. On the other hand, Wild et al. (1992) measured both  $^{12}\text{CO}(J=3-2)$  and  $^{13}\text{CO}(J=3-2)$  emission lines using the IRAM 30 m radio telescope in February 1992 and obtained both  $I[^{12}\text{CO}(J=3-2)] = 1334 \text{ K km s}^{-1}$  at  $(\Delta\alpha, \Delta\delta) = (-5, -5)$  and  $I[^{13}\text{CO}(J=3-2)] = 70.4 \text{ K km s}^{-1}$  at  $(\Delta\alpha, \Delta\delta) = (-7, -5)$  where  $\Delta\alpha$  and  $\Delta\delta$  are offsets from the nucleus position in right ascension and declination, respectively, in units of arcsec. Although the measured positions are slightly different, these measurements give an integrated intensity ratio,  $R_{3-2} \simeq 18.9$ . This together with the results by Tilanus et al. (1991) indicates that  $R_{3-2}$  in the nuclear region is  $\simeq 15 - 20$ . Since this value is nearly the same as the threshold value which defines the class of high- $R_{1-0}$  galaxies (TO98), it suggests that the  $J = 3$  transition is still not high enough to allow disentanglement of radiative transfer and abundance effects in M82.

As suggested by Taniguchi & Ohyama (1998b), it is possible that a large value of  $R$  can be attributed to the effect of superwind activity (i.e., the possible destruction of dense gas as well as dust grains, and the large velocity widths observed in the CO outflow). In fact, in M82,  $R_{3-2}$  is higher in the nuclear region than in the starburst ring (Tilanus et al. 1991).

Since M82 is indeed a superwind-starburst galaxy (Bland & Tully 1988), the higher  $R_{3-2}$  value in the nuclear region of M82 could possibly be due to superwind activity. However, Tilanus et al. (1991) suggested that intensity ratios of the three lowest transition lines of  $^{12}\text{CO}$  and  $^{13}\text{CO}$  can be explained if  $^{13}\text{CO}$  is overabundant with respect to  $^{12}\text{CO}$  just like what has been measured in the Galactic center, being contrary to our interpretation.

Another measurement of the  $^{13}\text{CO}(J=3-2)$  line was obtained at the central region of IC 342;  $R_{3-2} \simeq 7.7$  (Wall & Jaffe 1990). However, since the beam size of  $^{13}\text{CO}(J=3-2)$  observation (24 arcsec) is different from that of  $^{12}\text{CO}(J=3-2)$  one (15 arcsec), the above value may not be reliable.

Until more extragalactic  $\text{CO}(J=3-2)$  data is obtained it is clearly impossible to draw any firm conclusions about  $R_{3-2}$  in luminous starburst mergers as well as normal galaxies.

#### 4. DISCUSSION

We have shown that the  $R_{2-1}$  ratio is also high (typically  $> 20$ ) in the high- $R_{1-0}$  galaxies. Furthermore, the  $R_{3-2}$  value in the nuclear region of M82 suggests that this ratio may also be high in luminous starbursts, but this is only for one object. However, it is noted that the  $^{12}\text{CO}(J=3-2)/^{12}\text{CO}(J=1-0)$  integrated intensity ratio of starburst galaxies is often found to be higher than that in normal galaxies (e.g., Devereux et al. 1994 and references therein). Further, some nearby starburst galaxies such as M82 are detected in  $\text{CO}(J=4-3)$  (Güsten et al. 1993) and in  $\text{CO}(J=6-5)$  (Harris et al. 1992). The detection of these higher-transition CO lines suggests the presence of warm and dense gas clouds in starburst galaxies.

Although the kinetic gas temperature is not necessarily comparable to the dust temperature, it is interesting to compare molecular gas properties with the dust

temperature which is measured from the *IRAS* 60  $\mu\text{m}$  to 100  $\mu\text{m}$  flux ratio,  $S(60)/S(100)$ . In Figure 4, we compare  $R_{2-1}$  with  $S(60)/S(100)$  for the galaxies studied here. We also compare  $R_{1-0}$  with  $S(60)/S(100)$  for reference (the left panel). Though no tight correlation can be seen in either of these diagrams, we find that both  $R_{1-0}$  and  $R_{2-1}$  tend to increase with increasing  $S(60)/S(100)$ . This tendency suggests that the galaxies with higher dust temperatures have higher  $R$  values on the average. In the lower panels of Figure 4, we show comparisons of  $S(60)/S(100)$  with both  $L[{}^{12}\text{CO}(J=2-1)]/L[{}^{12}\text{CO}(J=1-0)]$  and  $L[{}^{13}\text{CO}(J=2-1)]/L[{}^{13}\text{CO}(J=1-0)]$  ratios. Interestingly, we find no correlation in both the diagrams. Average ratios of both  $L[{}^{12}\text{CO}(J=2-1)]/L[{}^{12}\text{CO}(J=1-0)]$  and  $L[{}^{13}\text{CO}(J=2-1)]/L[{}^{13}\text{CO}(J=1-0)]$  are  $0.81 \pm 0.17$  and  $1.15 \pm 0.71$ , respectively for the high  $R_{1-0}$  starburst mergers. Therefore, there seems to be no significant difference in the excitation toward  $J=2$  between  ${}^{12}\text{CO}$  and  ${}^{13}\text{CO}$ .

We also investigate whether a correlation exists between  $R_{1-0}$  and the luminosity ratio  $L[{}^{12}\text{CO}(J=2-1)]/L[{}^{12}\text{CO}(J=1-0)]$  for our sample (Figure 5). Since the high- $R_{1-0}$  mergers tend to have higher dust temperatures (see Table 2), it is likely that their CO kinetic temperatures are also higher than those of the normal- $R_{1-0}$  galaxies. These high temperatures could lead to both higher  $R_{1-0}$  and to higher  $L[{}^{12}\text{CO}(J=2-1)]/L[{}^{12}\text{CO}(J=1-0)]$  as demonstrated by large velocity gradient models (Sakamoto et al. 1994, 1997).

However, there is no such tendency as shown in Figure 5.

Finally, we investigate whether there is any relationship between  $R_{1-0}$ ,  $R_{2-1}$  and the  $L(\text{FIR})/L(\text{CO})$  ratio which is generally considered to give a measure of star formation efficiency. Figure 6 shows that the high- $R_{1-0}$  mergers as a group have a higher mean  $L(\text{FIR})/L(\text{CO})$  ratio as well as a higher mean  $R_{2-1}$  ratio than the “normal- $R_{1-0}$ ” galaxies. But, other than that there appears to be no clear correlation between either  $R_{1-0}$  or  $R_{2-1}$  with respect to  $L(\text{FIR})/L(\text{CO})$ . Therefore, we are led once again to suggest that

“superwinds” may be the best explanation for what produces the high- $R_{1-0}$  values. Indeed, it should be noted that nearly all of the high- $R_{1-0}$  galaxies show morphological and/or spectroscopic evidence for superwinds (Taniguchi & Ohyama 1998b). Both the abnormally large velocity gradients associated with these superwinds and the possible destruction of dense gas clouds by the dynamical effect of the superwind activity, could possibly combine to reduce the observed intensity of the much more optically thin  $^{13}\text{CO}$  in the lower- $J$  transitions relative to the  $^{12}\text{CO}$  emission. Further tests of this hypothesis will require measurements of the  $J \geq 3$  transitions of both  $^{12}\text{CO}$  and  $^{13}\text{CO}$  for the galaxies in Table 1.

We would like to thank Seiichi Sakamoto for useful discussions. YO was supported by a Grant-in-Aid for JSPS Fellows by the Ministry of Education, Science, Sports and Culture. This work was supported in part by the Ministry of Education, Science, Sports and Culture in Japan under Grant Nos. 07055044, 10044052, and 10304013.

## REFERENCES

Aalto, S., Black, J. H., Johansson, L. E. B., & Booth, R. S. 1991, A&A, 249, 323

Aalto, S., Booth, R. S., Black, J. H., & Johansson, L. E. B. 1995, A&A, 300, 369

Aalto, S., Radford, S. J. E., Scoville, N. Z., & Sargent, A. I. 1997, ApJ, 475, L107

Bland, J., & Tully, B. 1988, Nature, 334, 43

Casoli, F., Dupraz, C., & Combes, F. 1992a, A&A, 264, 49

Casoli, F., Dupraz, C., & Combes, F. 1992b, A&A, 264, 55

Casoli, F., Dupraz, C., Combes, F., & Kazès, I. 1991, A&A, 251, 1

de Vaucouleurs, G., de Vaucouleurs, A., Corwin, H. G. Jr., Buta, R. J., Paturel, G., & Fouqué, P. 1991, Third Reference Catalogue of Bright Galaxies (Springer-Verlag)

Devereux, N., Taniguchi, Y., Sanders, D. B., Nakai, N., & Young, J. S. 1994, AJ, 107, 2006

Freeman, K. C., Karlsson, B., Lynga, G., Burrell, J. F., van Woerden, H., & Goss, R. 1977, A&A, 55, 445

Garay, G., Mardones, D., & Mirabel, I. F. 1993, A&A, 277, 405

Güsten, R., Serabyn, E., Kasemann, C., Schinckel, A., Schneider, G., Schultz, A., & Young, K. 1993, ApJ, 402, 537

Helou, G. I., Soifer, B. T., & Rowan-Robinson, M. 1985, ApJ, 298, L7

Henkel, C., Chin, Y.-N., Mauersberger, R., & Whiteoak, J. B. 1998, A&A, 329, 443

Henkel, C., & Mauersberger, R. 1993, A&A, 274, 730

Henkel, C., Mauersberger, R., & Baan, W. A. 1991, A&ARv, 3, 47

Hurt, R. L., & Turner, J. L. 1991, ApJ, 377, 434

Lonsdale, C. J., Helou, G., Good, J. C., & Rice, W. 1989, Cataloged Galaxies and Quasars Observed in the *IRAS* Survey, Version 2, JPL D-1932 (Pasadena: JPL)

Moshir, M., et al. 1992, Explanatory Supplement to the *IRAS* Faint Source Survey, Version 2, JPL-D-10015 8/92 (Pasadena: JPL)

Sakamoto, S., Handa, T., Sofue, Y., Honma, M., & Sorai, K. 1997, ApJ, 475, 134

Sakamoto, S., Hayashi, M., Hasegawa, T., Handa, T., & Oka, T. 1994, ApJ, 425, 641

Sanders, D. B., Egami, E., Lipari, S., Mirabel, I. F., & Soifer, B. T. 1995, AJ, 110, 1993

Strauss, M. A., Huchra, J. P., Davis, M., Yahil, A., Fisher, K. B., & Tonry, J. 1992, ApJS, 83, 29

Taniguchi, Y., & Ohyama, Y. 1998a, ApJ, 507, L121 (TO98)

Taniguchi, Y., & Ohyama, Y. 1998b, ApJ, 508, L13

Tilanus, R. P. J., et al. 1991, ApJ, 376, 500

Tully, R. B. 1988, *Nearby Galaxies Catalog* (Cambridge University Press)

Turner, J. L., & Hurt, R. L. 1992, ApJ, 384, 72

Wall, W. F., & Jaffe, D. T. 1990, ApJ, 365, L45

Wild, W., Harris, A. L., Eckart, A., Genzel, R., Graf, U. U., Jackson, J. M., Russel, A. P. G., & Stutzki, J. 1992, A & A, 265, 447

Young, J. S., & Scoville, N. Z. 1991, ARA&A, 29, 581

Fig. 1.— Diagram of  $L[{}^{12}\text{CO}(J=2-1)]$  vs.  $L[{}^{13}\text{CO}(J=2-1)]$  (right panel). For reference, we also show a diagram of  $L[{}^{12}\text{CO}(J=1-0)]$  vs.  $L[{}^{13}\text{CO}(J=1-0)]$  taken from TO98 (left panel). The high- $R$  galaxies ( $R_{1-0} \geq 20$ ) are shown by filled circles.

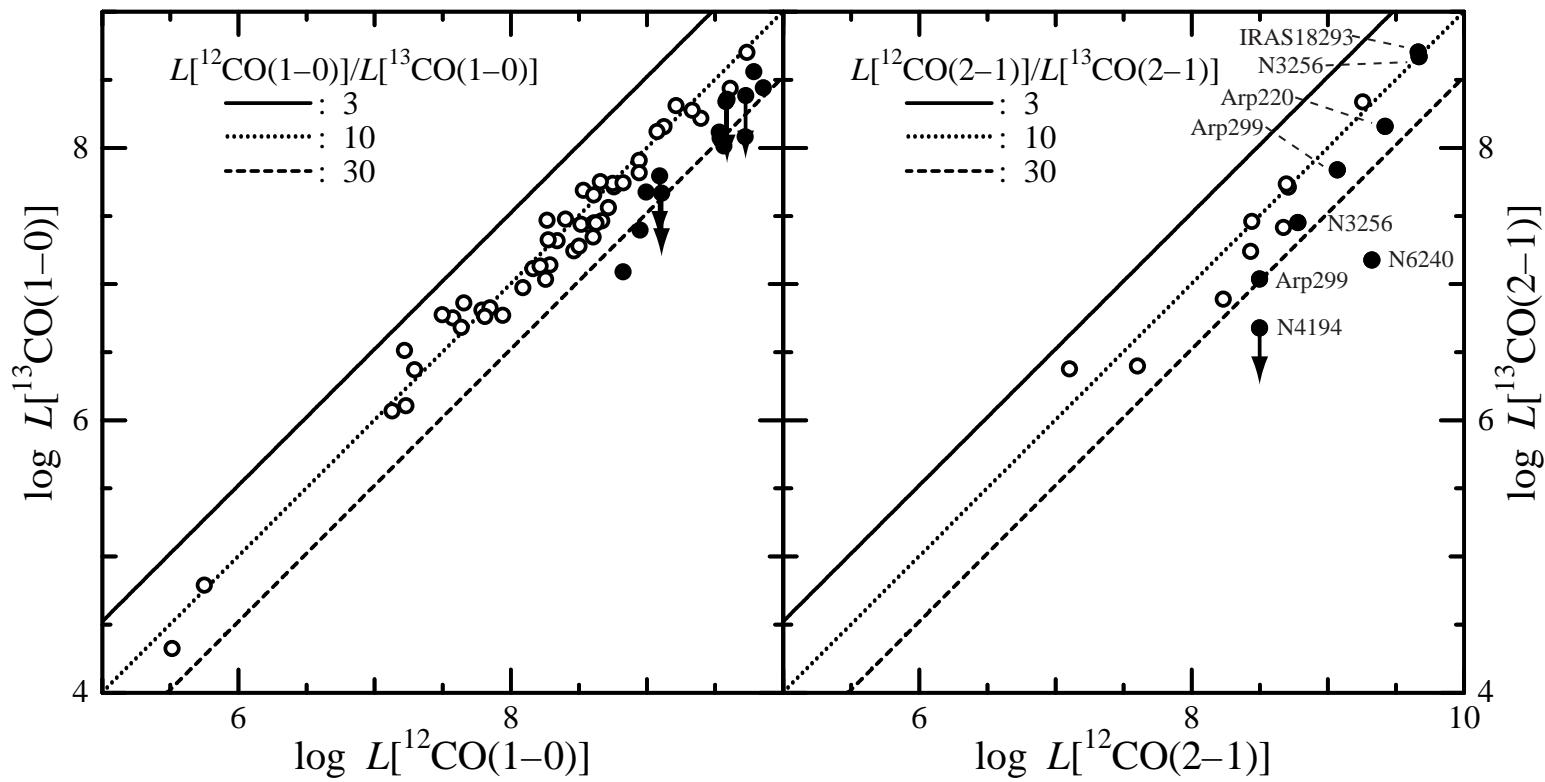
Fig. 2.— Diagrams of  $R_{2-1}$  (top),  $L[{}^{12}\text{CO}(J=2-1)]$  (middle), and  $L[{}^{13}\text{CO}(J=2-1)]$  (bottom) against  $L(\text{FIR})$ . The symbols have the same meaning as those in Figure 1. Alphabets in the upper panel mean; a: NGC 6240, b: NGC 4194, c: Arp 299, d: NGC 3256, e: Arp 220, and f: IRAS 18293–3413.

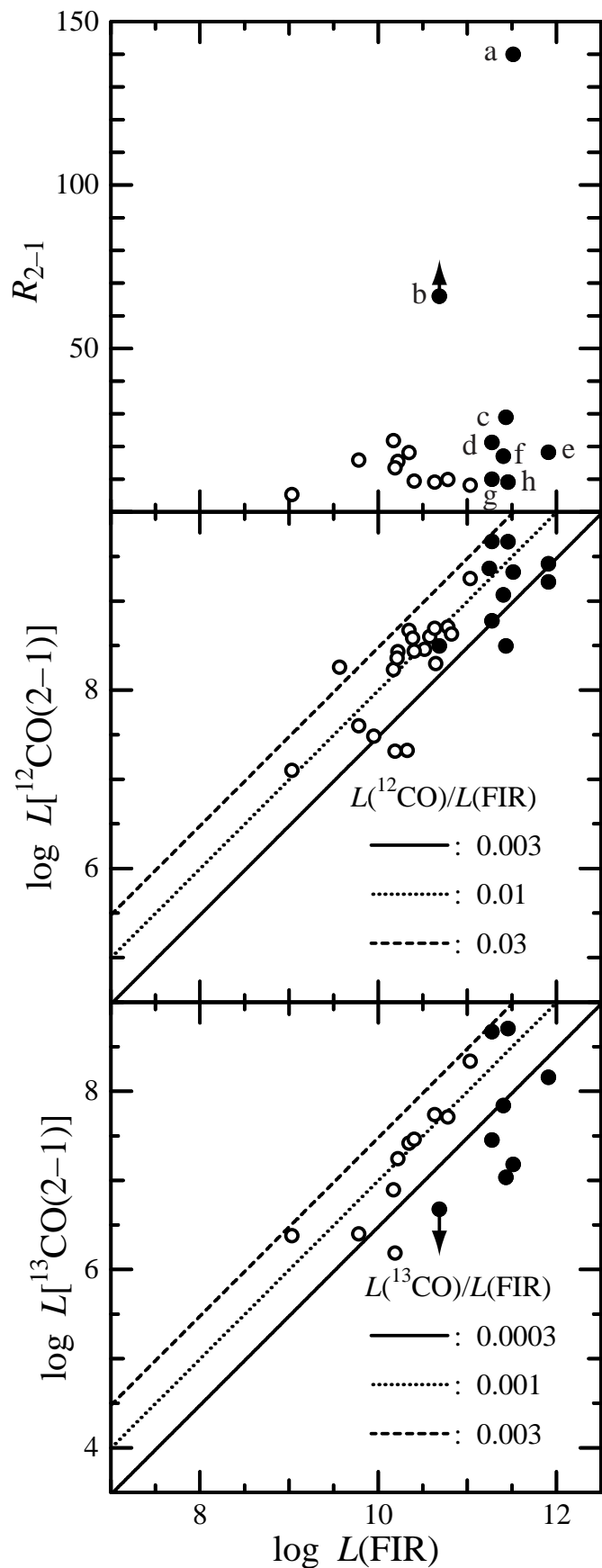
Fig. 3.— Diagram of  $R_{2-1}$  vs.  $R_{1-0}$ . The symbols have the same meaning as those in Figure 1.

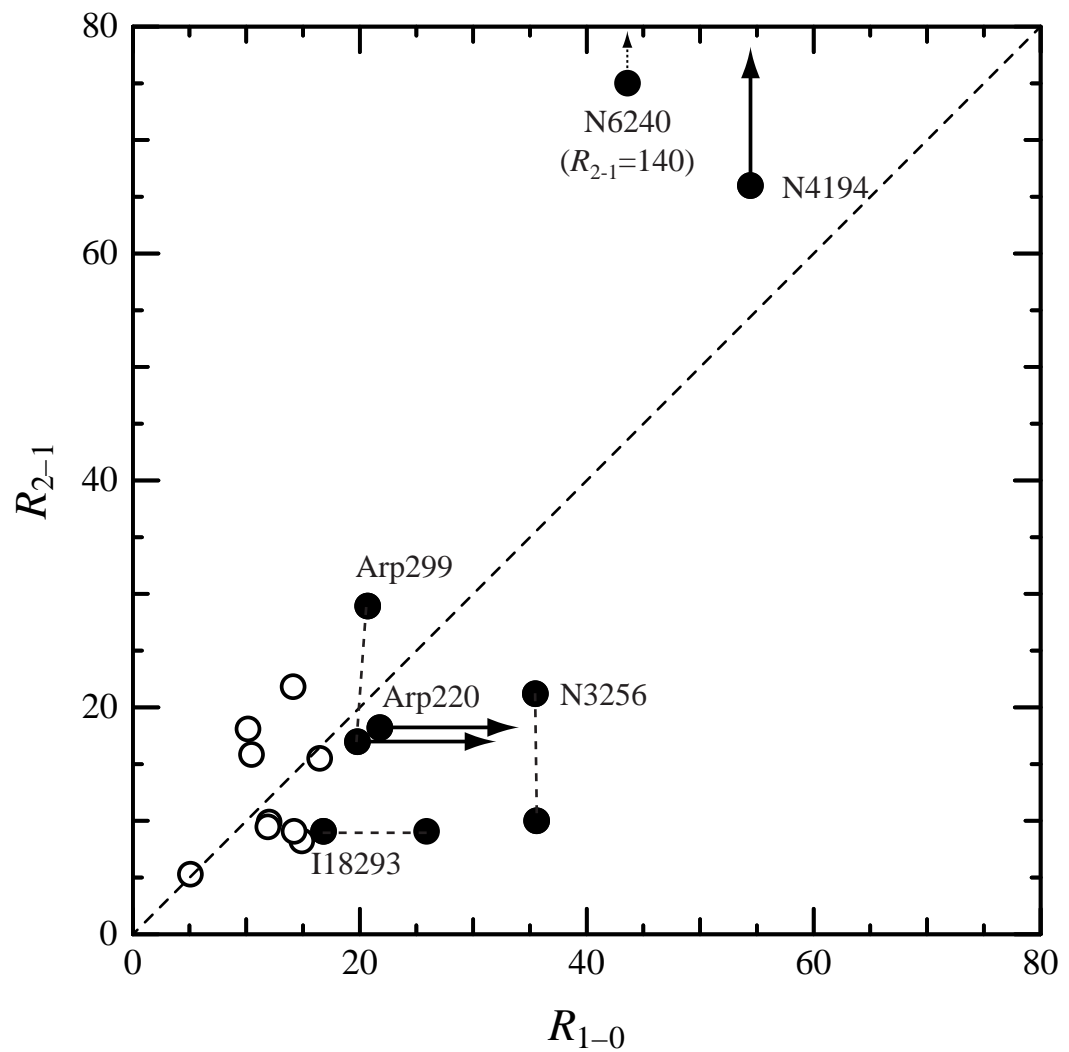
Fig. 4.— Diagrams of  $R_{2-1}$  (upper right),  $R_{1-0}$  (upper left),  ${}^{12}\text{CO}(J=2-1)$  to  ${}^{12}\text{CO}(J=1-0)$  luminosity ratio (lower right), and  ${}^{13}\text{CO}(J=2-1)$  to  ${}^{13}\text{CO}(J=1-0)$  luminosity ratio (lower left) against  $S(60)/S(100)$ . Note that  $R_{2-1} = 140$  for NGC 6240. The data of  $R_{1-0}$  are taken from TO98. Alphabets in the upper left panel mean; a: NGC 4194, b: NGC 6240, c: NGC 3256, d: NGC 3256, e: NGC 1614, f: NGC 3256, g: IRAS 18293–3413, h: NGC 3256, i: Arp 220, j: Arp 299, k: Arp 299, l: IRAS 18293–3413, m: ESO 541-IG 23, and n: Arp 220.

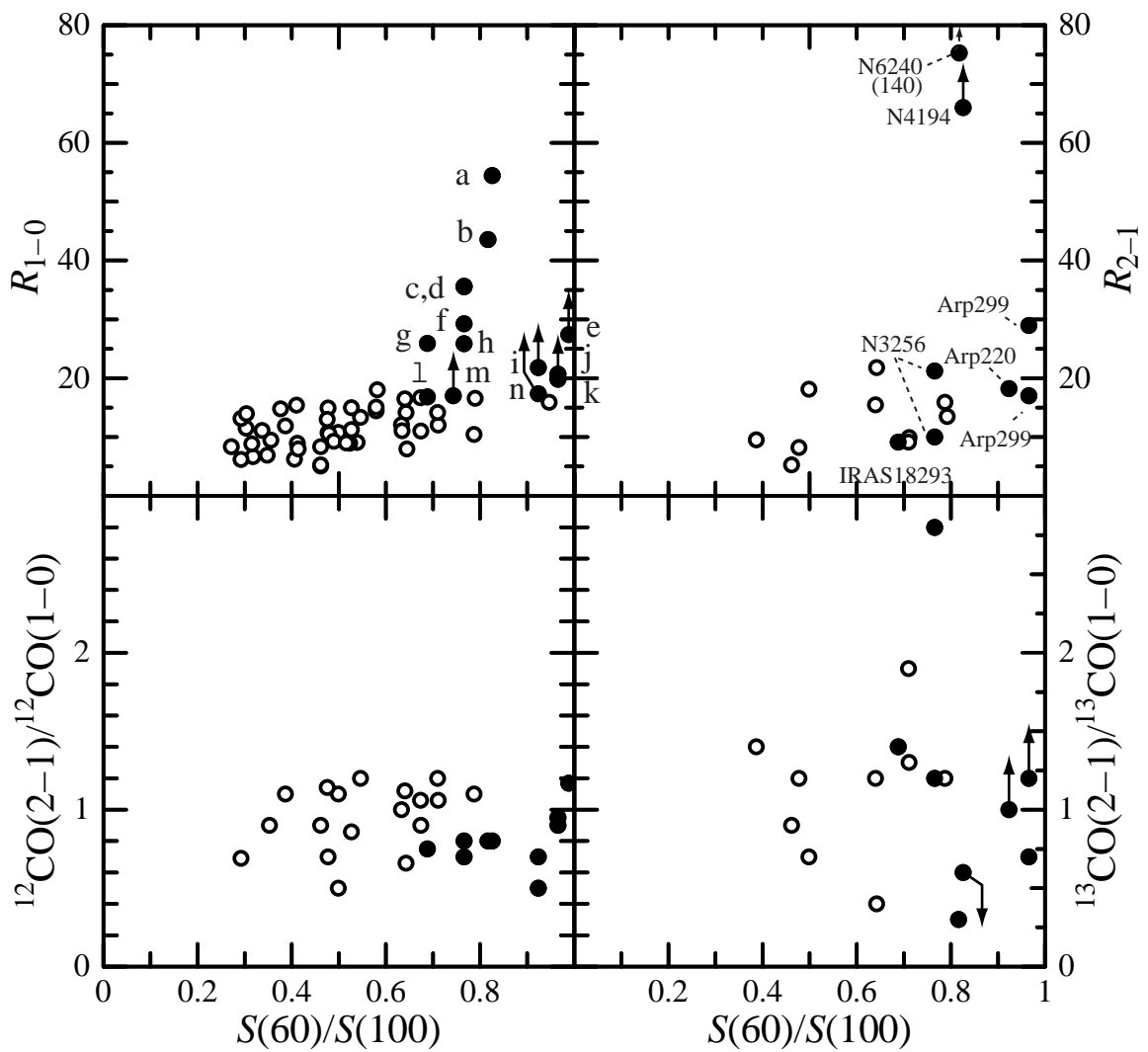
Fig. 5.— Diagram of  $R_{1-0}$  vs.  ${}^{12}\text{CO}(J=2-1)$  to  ${}^{12}\text{CO}(J=1-0)$  integrated intensity ratio. The symbols have the same meaning as those in Figure 1. The large velocity gradient models taken from Sakamoto et al. (1997) are shown for the case of  $X(\text{CO})/dv/dr = 10^{-5} [\text{km s}^{-1} \text{pc}^{-1}]^{-1}$  where  $X(\text{CO})$  is the fractional abundance of  ${}^{12}\text{CO}$  and  $dv/dr$  is the velocity gradient. Kinetic temperatures and densities of molecular gas are labeled.

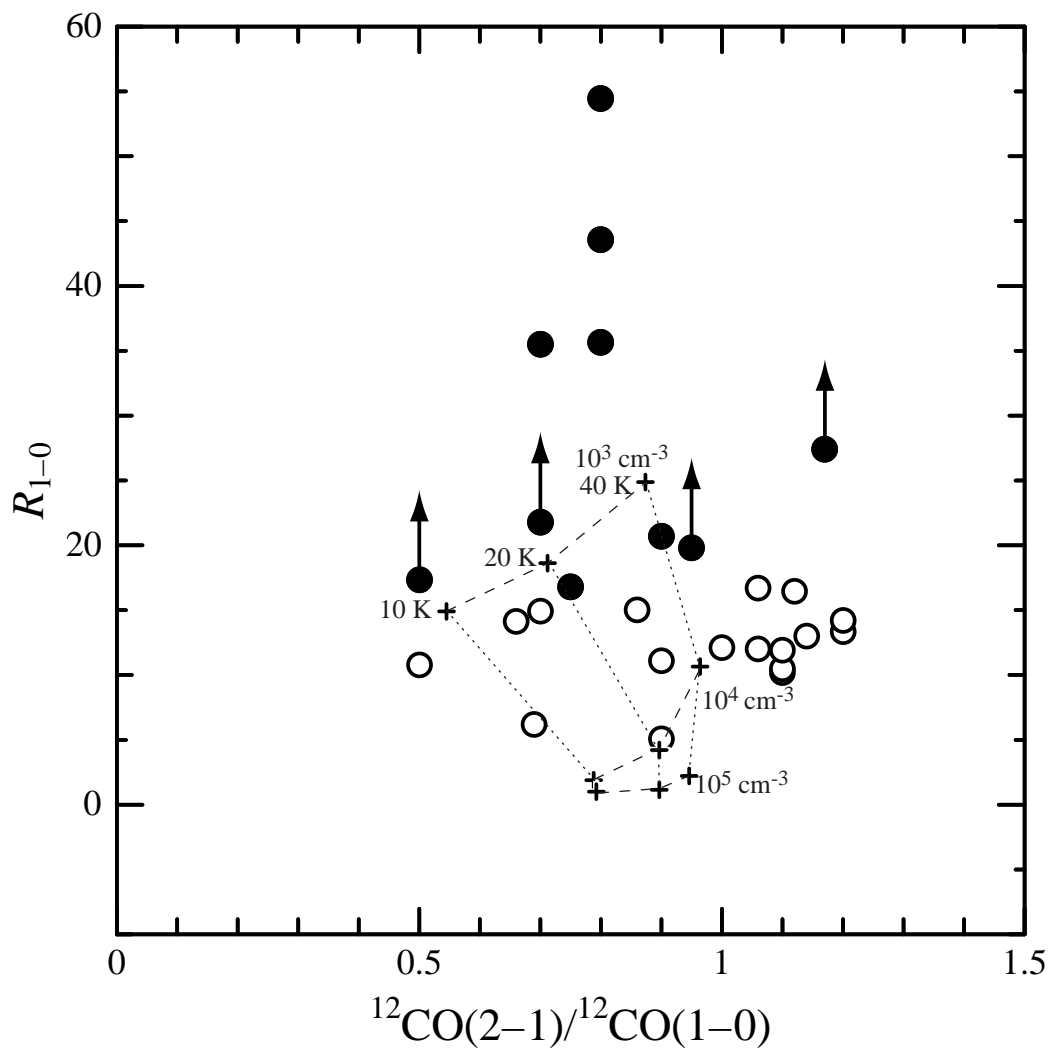
Fig. 6.— Diagrams of  $R_{1-0}$  and  $R_{2-1}$  against  $L(\text{FIR})/L(\text{CO})$  ratio. The symbols have the same meaning as those in Figure 1. Note that the data shown in the left panel are taken from TO98.











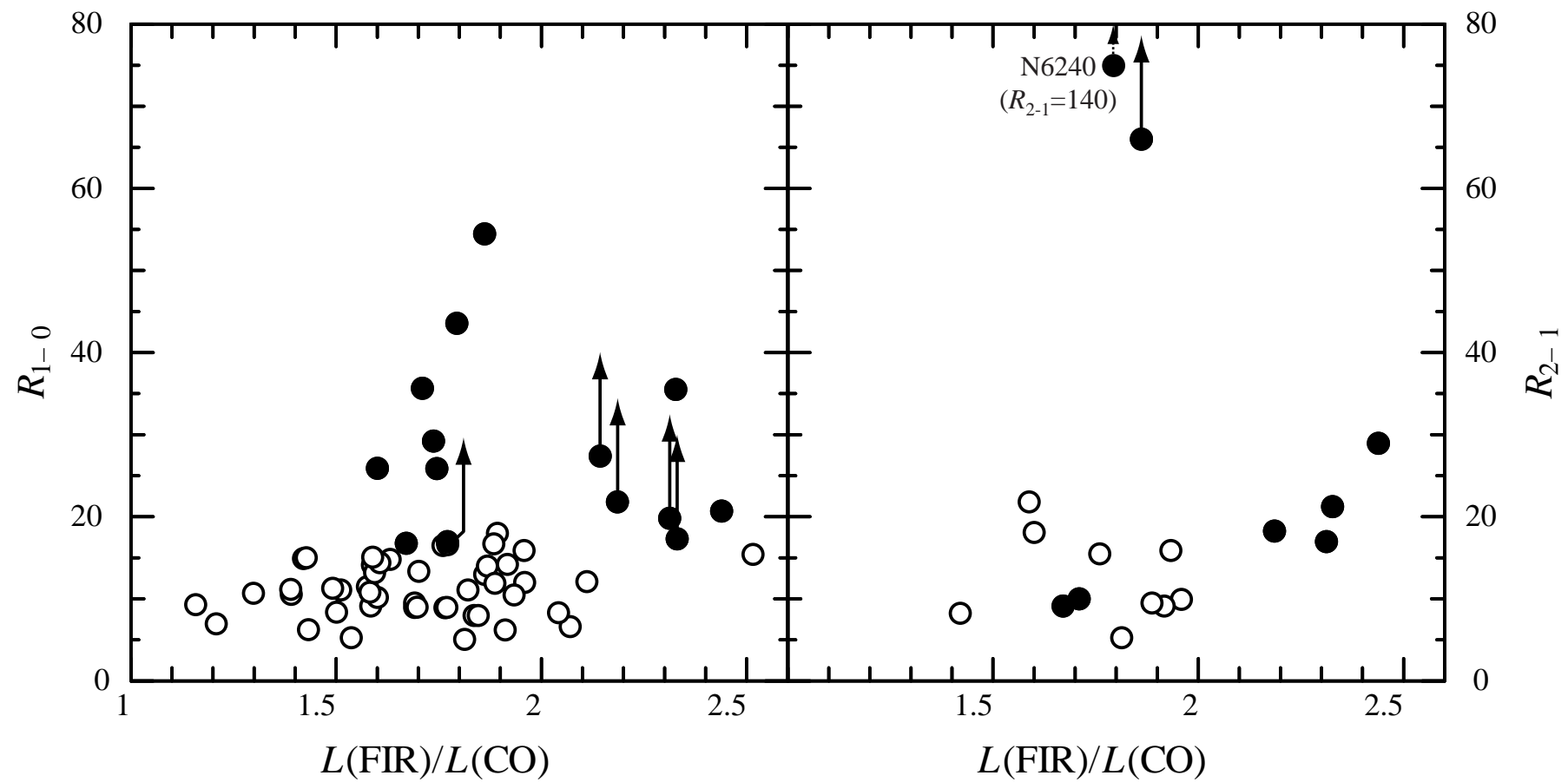


Table 1. Properties of the sample of galaxies

(1)	(2)	(3)	(4)	(5)	(6)	(7)	(8)	(9)	(10)	(11)	(12)	(13)
N520	28	8.76	7.71	8.60	...	0.674	10.58	11.0	...	0.9	...	1
N660	12	8.58	7.43	8.23	6.89	0.643	10.17	14.1	21.8	0.7	0.4	1
N828	73 <sup>a</sup>	9.61	8.44	9.25	8.34	0.477	11.03	14.9	8.2	0.7	1.2	2
N986	23	8.75	7.74	8.67	7.42	0.499	10.35	10.2	18.1	1.1	0.7	1
N1614	62 <sup>a</sup>	9.11	< 7.67	9.37	...	0.988	11.25	> 27.4	...	1.2	...	1
N1808	11	8.46	7.25	8.43	7.24	0.640	10.22	16.5	15.5	1.1	1.2	1
N2146	17	8.82	7.74	8.71	7.71	0.711	10.78	12.0	9.9	1.1	1.3	1
N2369	44 <sup>a</sup>	9.39	8.22	8.63	...	0.527	10.82	15.0	...	0.9	...	1
N3079	20	8.94	7.91	8.46	...	0.499	10.52	10.8	...	0.5	...	1
NGC 3256	37	8.95	7.40	8.78	7.45	...	...	35.5	21.2	0.7	1.2	2
N4038/9	25	8.94	7.82	8.30	...	0.546	10.64	13.3	...	1.2	...	1
N4194	39	8.83	7.09	8.50	< 6.68	0.826	10.69	54.4	> 66.0	0.8	< 0.6	2
N4826	4	7.22	6.51	7.10	6.38	0.461	9.03	5.1	5.3	0.9	0.9	1
N5055	7	7.65	6.86	8.26	...	0.292	9.57	6.2	...	0.7	...	1
N6215	21	8.21	7.13	7.32	...	0.633 <sup>b</sup>	10.33 <sup>b</sup>	12.1	...	1.0	...	1
N6240	98 <sup>a</sup>	9.72	8.08	9.32	7.18	0.816	11.52	43.6	140	0.8	0.3	2
N6951	24	8.40	...	8.36	...	0.353	10.21	...	...	0.9	...	1
N7552	20	8.72	7.56	8.70	7.74	0.710	10.63	14.2	9.1	1.2	1.9	1
N7582	18	8.50	7.28	8.58	...	0.673	10.39	16.7	...	1.1	...	1
IC2554	17	8.09	6.97	7.48	...	0.475	9.95	13.0	...	1.1	...	1
U2855	20	8.52	7.44	8.44	7.46	0.387	10.40	11.9	9.5	1.1	1.4	1
U2866	16 <sup>c</sup>	...	...	7.32	6.19	0.792	10.19	...	13.5	...	...	1
Circinus	4 <sup>d</sup>	7.85	6.83	7.60	6.40	0.787 <sup>e</sup>	9.78 <sup>e</sup>	10.5	15.9	1.1	1.2	1
Arp 220	74 <sup>a</sup>	9.72	< 8.39	9.42	8.16	...	...	> 21.8	18.2	0.7	> 1.0	2
Arp 299	42 <sup>a</sup>	8.99	7.68	8.50	7.04	...	...	20.7	28.9	0.9	0.7	2
I18293 <sup>f</sup>	73 <sup>c</sup>	9.79	8.56	9.66	8.70	0.688	11.46	16.8	9.1	1.8	1.4	1

Note. — (1) Name, (2) Distance (Mpc) taken from Tully (1988), (3)  $\log L[{}^{12}\text{CO}(J = 1 - 0)]$  (K km s $^{-1}$  pc $^2$ ), (4)  $\log L[{}^{13}\text{CO}(J = 1 - 0)]$  (K km s $^{-1}$  pc $^2$ ), (5)  $\log L[{}^{12}\text{CO}(J = 2 - 1)]$  (K km s $^{-1}$  pc $^2$ ), (6)  $\log L[{}^{13}\text{CO}(J = 2 - 1)]$  (K km s $^{-1}$  pc $^2$ ), (7)  $S(60)/S(100)$ , (8)  $L(\text{FIR})$  ( $L_{\odot}$ ), (9)  $R_{1-0}$ , (10)  $R_{2-1}$ , (11)  $L[{}^{12}\text{CO}(J = 2 - 1)]/L[{}^{12}\text{CO}(J = 1 - 0)]$ , (12)  $L[{}^{13}\text{CO}(J = 2 - 1)]/L[{}^{13}\text{CO}(J = 1 - 0)]$ , and (13) Reference.

<sup>a</sup>Estimated using a Hubble constant  $H_0 = 75$  km s $^{-1}$  Mpc $^{-1}$  with  $V_{\text{GSR}}$  given in de Vaucouleurs et al. (1991). <sup>b</sup>Sanders et al. (1995) <sup>c</sup>Strauss et al. (1992) <sup>d</sup>Freeman et al. (1977) <sup>e</sup>Lonsdale et al. (1989) <sup>f</sup>I18293 = IRAS 18293–3413

References. — (1) Aalto et al. 1995; (2) Casoli et al. 1992

Table 2. Comparisons of physical properties between the high- $R_{1-0}$  mergers and the normal- $R_{1-0}$  galaxies

	Units	High- $R_{1-0}$ mergers	Normal- $R_{1-0}$ galaxies
$R_{1-0}$		$31.5 \pm 12.7$	$12.2 \pm 3.2$
$R_{2-1}$		$47.3 \pm 45.2$	$12.7 \pm 4.9$
$\log L[{}^{12}\text{CO}(J=1-0)]$	$(L_\odot)$	$9.30 \pm 0.39$	$8.50 \pm 0.63$
$\log L[{}^{13}\text{CO}(J=1-0)]$	$(L_\odot)$	$7.87 \pm 0.34$	$7.44 \pm 0.52$
$\log L(\text{FIR})$	$(L_\odot)$	$11.36 \pm 0.34$	$10.26 \pm 0.53$
$\log L(\text{FIR})/L[{}^{12}\text{CO}(J=1-0)]$		$2.06 \pm 0.27$	$1.76 \pm 0.18$
$T_d$	(K)	$44.4 \pm 2.6$	$38.2 \pm 3.6$